Disruption of vitellogenesis and spermatogenesis by triclabendazole (TCBZ) in a TCBZ-resistant isolate of *Fasciola hepatica* following incubation *in vitro* with a P-glycoprotein inhibitor

J. SAVAGE, M. MEANEY, G. P. BRENNAN, E. HOEY, A. TRUDGETT *and* I. FAIRWEATHER*

Parasite Therapeutics Research Group, School of Biological Sciences, Medical Biology Centre, The Queen's University of Belfast, 97 Lisburn Road, Belfast, BT9 7BL, Northern Ireland

(*Received 22 September 2013; revised 28 November 2013 and 23 January 2014; accepted 11 February 2014; first published online 24 April 2014*)

SUMMARY

A study has been carried out to investigate whether the action of triclabendazole (TCBZ) against *Fasciola hepatica* is altered by inhibition of P-glycoprotein (Pgp)-linked drug efflux pumps. The Sligo TCBZ-resistant fluke isolate was used for these experiments and the Pgp inhibitor selected was R(+)-verapamil [R(+)-VPL]. In the first experiment, flukes were initially incubated for 2 h in R(+)-VPL (100 μM), then incubated in R(+)-VPL + triclabendazole sulphoxide (TCBZ.SO) (50 μg mL^{-1}, or 133·1 μM) until flukes ceased movement (at 9 h post-treatment). In a second experiment, flukes were incubated in TCBZ.SO alone and removed from the incubation medium following cessation of motility (after 15 h). In the third experiment, flukes were incubated for 24 h in R(+)-VPL on its own. Changes to the testis tubules and vitelline follicles following drug treatment and following Pgp inhibition were assessed by means of light microscope histology and transmission electron microscopy. Incubation of the Sligo isolate in either R(+)-VPL or TCBZ.SO on their own had a limited impact on the morphology of the two tissues. Greater disruption was observed when the drugs were combined, in terms of the block in development of the spermatogenic and vitelline cells and the apoptotic breakdown of the remaining cells. Sperm formation was severely affected and abnormal. Large spaces appeared in the vitelline follicles and synthesis of shell protein was disrupted. The results of this study support the concept of altered drug efflux in TCBZ-resistant flukes and indicate that drug transporters may play a role in the development of drug resistance.

Key words: *Fasciola hepatica*, liver fluke, triclabendazole resistance, R(+)-verapamil, P-glycoprotein, transmission electron microscopy.

INTRODUCTION

One mechanism adopted by helminth parasites to resist the action of anthelmintics is the enhanced activity of drug efflux pumps, linked to transporter molecules such as P-glycoprotein (Pgp) (Kerboeuf *et al*. 2003*a*; Wolstenholme *et al*. 2004; Prichard and Roulet, 2007; Lespine *et al*. 2012). The phenomenon is well documented in nematodes (e.g. Xu *et al*. 1998; Molento and Prichard, 1999; Stitt *et al*. 2011; Tompkins *et al*. 2011). Among trematodes, over-expression of Pgp in schistosomes has been linked to resistance against praziquantel (James *et al*. 2009; Messerli *et al*. 2009; Kasinathan *et al*. 2010*a*, *b*, 2011; Kasinathan and Greenberg, 2012).

This study is on another trematode, *Fasciola hepatica*, and is part of a wider investigation examining the role of altered Pgp activity in the development of resistance to triclabendazole (TCBZ). It has been shown that the concentrations of TCBZ and its sulphoxide metabolite (TCBZ.SO) are lower in the TCBZ-resistant (TCBZ-R) Sligo isolate than in the TCBZ-susceptible (TCBZ-S) Cullompton isolate following incubation of flukes in the two compounds, a result which was attributed to an increased expression and action of Pgp-linked efflux pumps (Alvarez *et al*. 2005; Mottier *et al*. 2006). The effect was reversed by co-incubation with Pgp inhibitors and the response was specific to TCBZ, as it was not evident with albendazole, a related benzimidazole drug (Mottier *et al*. 2006). In another TCBZ-R isolate, the Dutch isolate, an amino acid substitution in a Pgp gene has been identified and it may be linked to TCBZ resistance (Wilkinson *et al*. 2012). Two previous scanning electron microscope (SEM) studies involving TCBZ-R flukes (the Oberon and Sligo isolates) have shown that co-incubation of flukes in TCBZ.SO + the Pgp inhibitor, R(+)-verapamil [R(+)-VPL] led to greater surface disruption of the flukes than treatment with TCBZ.SO alone (Meaney *et al*. 2013; Savage *et al*. 2013*a*). A similar potentiation of drug activity was

* Corresponding author: School of Biological Sciences, Medical Biology Centre, The Queen's University of Belfast, 97 Lisburn Road, Belfast, BT9 7BL, Northern Ireland. E-mail: i.fairweather@qub.ac.uk

doi:10.1017/S0031182014000377

not seen with the Cullompton isolate. Moreover, the combination treatment significantly reduced the time taken for TCBZ.SO to immobilize the flukes, particularly in the TCBZ-R isolates (Meaney *et al*. 2013; Savage *et al*. 2013*a*). A follow-up transmission electron microscope (TEM) study on the Sligo isolate determined the internal changes in the tegument (and gut) that caused the changes visible externally and the results supported the conclusion to the SEM study, in terms of the enhancement of drug action (Savage *et al*. 2013*b*). The present study focuses on two key components of the reproductive system, namely, the testis and vitellaria. They are particularly sensitive to drug action and have often been used as models of drug action (see Toner *et al*. 2011*a*, *b* for references). The results highlight the impact of Pgp inhibition on the reproductive potential of TCBZ-treated TCBZ-R flukes.

The Pgp inhibitor chosen was (R+)-VPL. VPL is an established inhibitor of Pgp-mediated drug efflux (Pereira *et al*. 1995; Toffoli *et al*. 1995; Tiberghien and Loor, 1996; Choi *et al*. 1998; Biscardi *et al*. 2006). The R(+) isomer was used rather than the S(−) isomer of VPL or racemic VPL [a mixture of (+) and (−) isomers]. This was because it is equally or more specific for Pgp than the other two forms of VPL but, more importantly, it is 10-fold less active as a calcium channel antagonist than S(−)-VPL (Echizen *et al*. 1985; Ye and Van Dyke, 1988; Höllt *et al*. 1992; Varma *et al*. 2003). In terms of avoiding changes to fluke motility (which, in turn, might impact on morphology), this was an important precaution to take, as racemic VPL at an equivalent concentration (100 μM) has been shown to induce paralysis of the whole fluke (Holmes, 1983; Chapter 6, figs 6·5 and 6·7) and affect the contractility of isolated fluke muscle strips (Wells, 2008; Chapter 5, fig. 5·4). In contrast, R(+)-VPL did not affect motility over a 24-h period (Savage *et al*. 2013*a*).

MATERIALS AND METHODS

The protocol for this investigation was the same as that used for the TEM study that focused on the tegument and gut of *F. hepatica* following Pgp inhibition (Savage *et al*. 2013*b*); the reader is referred to that publication for full details. Briefly, adult flukes of the Sligo TCBZ-R isolate were used for the experiments; for the provenance of the Sligo isolate, see the review by Fairweather (2011). Adult flukes were recovered from the bile duct of infected rats under sterile conditions in a laminar flow cabinet. Flukes were then washed in several changes of warm (37 °C) sterile NCTC 135 culture medium containing antibiotics (penicillin 50 IU mL^{-1}; streptomycin, 50 μg mL^{-1}) (NCTC 135 was obtained from Flow laboratories, Thame, Oxfordshire, UK; antibiotics were obtained from Sigma-Aldrich Co. Ltd., Poole, Dorset, UK). They were then subjected to one of three different drug treatments, as indicated below. Six flukes were incubated per treatment, with 4 being prepared for TEM and 2 for light microscopy.

In the first experiment, flukes were initially incubated for 2 h at 37 °C in R(+)-VPL (100 μM) alone, then incubated in a combination of R(+)-VPL (100 μM) + triclabendazole sulphoxide (TCBZ.SO) (at a concentration of 50 μg mL^{-1}, or 133·1 μM) until flukes ceased movement (at 9 h post-treatment: Savage *et al*. 2013*a*). TCBZ.SO was initially prepared as a stock solution in dimethyl sulphoxide (DMSO) and added to the culture medium to give a final solvent concentration of 0·1% (v/v); a stock solution of R(+)-VPL was initially prepared at a concentration of 1×10^{-1} M in distilled water.

In the second experiment, flukes were incubated at 37 °C in NCTC containing TCBZ.SO on its own at a concentration of 50 μg mL^{-1} and then removed from the incubation medium following cessation of motility (after 15 h: Savage *et al*. 2013*a*). A concentration of 50 μg mL^{-1} is the highest concentration that has been used in *in vitro* experiments and, at this concentration, the drug causes little disruption to tegumental morphology and no diminution of tubulin staining in the Sligo isolate over a 24-h period (Robinson *et al*. 2002; see also Savage *et al*. 2013*a*, *b*).

In the third experiment, flukes were incubated at 37 °C for 24 h in NCTC containing 100 μM R(+)-VPL on its own. At this concentration, there was no change in motility after 24 h incubation, nor any change in the fine structure of the tegument or gut (Savage *et al*. 2013*a*, *b*).

Untreated NCTC controls

Flukes were removed from the bile duct and briefly washed in warm (37 °C) sterile NCTC 135 culture medium (pH 7·4) containing antibiotics (penicillin, 50 IU mL^{-1}; streptomycin, 50 μg mL^{-1}). They were then incubated in NCTC culture medium containing 0·1% (v/v) DMSO at 37 °C for 24 h. 0 h controls were also prepared: the flukes were fixed immediately following their recovery from infected rats.

JB4 tissue preparation

Flukes were lightly flat-fixed for 30 min in 4% (w/v) paraformaldehyde (PFA) in 0·1 M phosphate buffered saline (PBS), pH 7·2, at room temperature. Each fluke was transected in three places to isolate the oral cone region, the anterior midbody region, the posterior midbody region and the tail region. Each section was free-fixed in 4% (w/v) PFA in 0·1 M PBS, pH 7·2, at room temperature for 4–6 h. The fluke sections were then washed overnight in 0·1 M PBS, pH 7·2, and dehydrated through an ascending series of alcohols. The sections were then infiltrated and embedded in JB4 resin. Sections 4 μm in thickness were cut on a pyramitome and mounted

https://doi.org/10.1017/S0031182014000377 Published online by Cambridge University Press

on multi-welled slides. The sections were stained with toluidine blue and examined under a light microscope.

Tissue preparation for transmission electron microscopy

Flukes were lightly flat-fixed for 1 h in 4% (w/v) glutaraldehyde in 0·1 M sodium cacodylate buffer (pH 7·4) containing 3% (w/v) sucrose at room temperature. Flukes were then sectioned into apical cone, midbody and tail regions. The apical cone region was divided into two parts, the midbody region was divided into the anterior and posterior midbody regions, and the tail region was sectioned into two parts. Each body section was further sub-divided into transverse sections approximately 2 mm in width. The sections were placed in fresh fixative for 3 h at room temperature and then washed in 0·1 M sodium cacodylate buffer (pH 7·4) containing 3% (w/v) sucrose and left overnight at 4 °C. Specimens were post-fixed in 1% osmium tetroxide for 1 h, washed in fresh buffer, dehydrated through an ascending series of ethanol and infiltrated and embedded in agar resin. Ultrathin sections, 60–70 nM in thickness, were cut on a Reichert Ultracut E ultramicrotome, placed onto sterile 200-mesh copper grids and stained with uranyl acetate (8 min) and lead citrate (5 min). Sections were examined in an FEI CM100 TEM which was operated at 100 keV.

RESULTS

Testis histology

For those readers not familiar with the characteristic features of the different stages in sperm formation, a brief description will be included here. There are three generations of spermatogonia, the tertiary spermatogonia forming a group of four cells, though they are not joined together. The spermatogonial cells typically lie at the periphery of the testis tubule, have a high nucleo-cytoplasmic ratio and are highly basophilic. Division of the tertiary spermatogonia produces a rosette of eight primary spermatocytes, joined together by a common cytoplasm. A distinctive feature of these cells at the EM level is the presence of synaptonemal complexes in the nucleus; they represent the pairing of homologous chromosomes at zygotene during meiotic prophase. The 16-cell secondary spermatocyte stage (also a rosette) is rarely seen. Once meiosis is complete, the 32-cell spermatid stage is reached. These cells undergo marked changes to form the spermatozoa: the changes include the elongation and differentiation of the nucleus and the formation of the axonemes that come to lie within the spermatozoa. Once formed, the latter break away from the residual cytoplasm and lie free within the lumen of the testis tubule. For a more detailed description of the various cell types, see Stitt and Fairweather (1990).

The histological profile of the testis of untreated 0 and 24 h control flukes from the TCBZ-resistant Sligo isolate showed a normal morphology, corresponding to that previously described by Hanna *et al*. (2008, Figs 3d and e; see also McConville *et al*. 2010; Hanna *et al*. 2013). All cell types (from spermatogonia to spermatozoa) were present within the tubule. Primary and secondary spermatogonia were present at the periphery of the tubule, and tertiary spermatogonia remained in close proximity. The later stages of spermatogenesis, namely, the primary spermatocytes, spermatids and spermatozoa were more centrally located in the tubule (Fig. 1A). Therefore, no abnormalities were observed following *in vitro* incubation. After 24 h incubation, R(+)-VPL (100 μM)-treated flukes appeared to have a normal testis profile, with all stages of spermatogenesis present, including mature spermatozoa and an abundance of primary and secondary spermatogonia at the periphery of the tubule (Fig. 1B). After treatment with TCBZ.SO (50 μg mL^{-1}) until inactivity at 15 h, flukes showed a normal testis profile, with all stages of spermatogenesis present in the tubules. An abundance of primary and secondary spermatogonia were located at the periphery of the tubule, and many mature spermatozoa were seen throughout the tubules (Fig. 1C and D). After treatment with a combination of R(+)-VPL (100 μM) + TCBZ.SO (50 μg mL^{-1}) until inactivity at 9 h, the testis tubules showed a marked reduction in the number of cells generally, resulting in an increase in 'empty' space within the tubule. There were few spermatogonia present. The intermediate stages of sperm development, viz. primary and secondary spermatocytes, were present. Apoptotic bodies containing irregular clumps of dense chromatin were present in the tubules; these bodies are due to missegregation during meiotic division in primary spermatocytes, which leads to apoptosis and ultimately cell death (Kumar *et al*. 2005). No spermatids or mature spermatozoa were visible in the testis tubule after combination treatment (Fig. 1E and F).

Testis ultrastructure

The ultrastructure of the testis in the 24 h control specimens retained a normal morphology (and was similar to the 0 h controls): it corresponded to the images presented by Stitt and Fairweather (1990) (Figs 1–6) and by McConville *et al*. (2010, Figs 5–7). Thus, no abnormalities in the spermatogenic cells of *F. hepatica* were observed following incubation *in vitro*.

Treatment for 24 h with R(+)-VPL (100 μM)

All stages of sperm development were present. Primary and secondary spermatogonia were abundant and situated in layers beneath the peripheral wall

https://doi.org/10.1017/S0031182014000377 Published online by Cambridge University Press

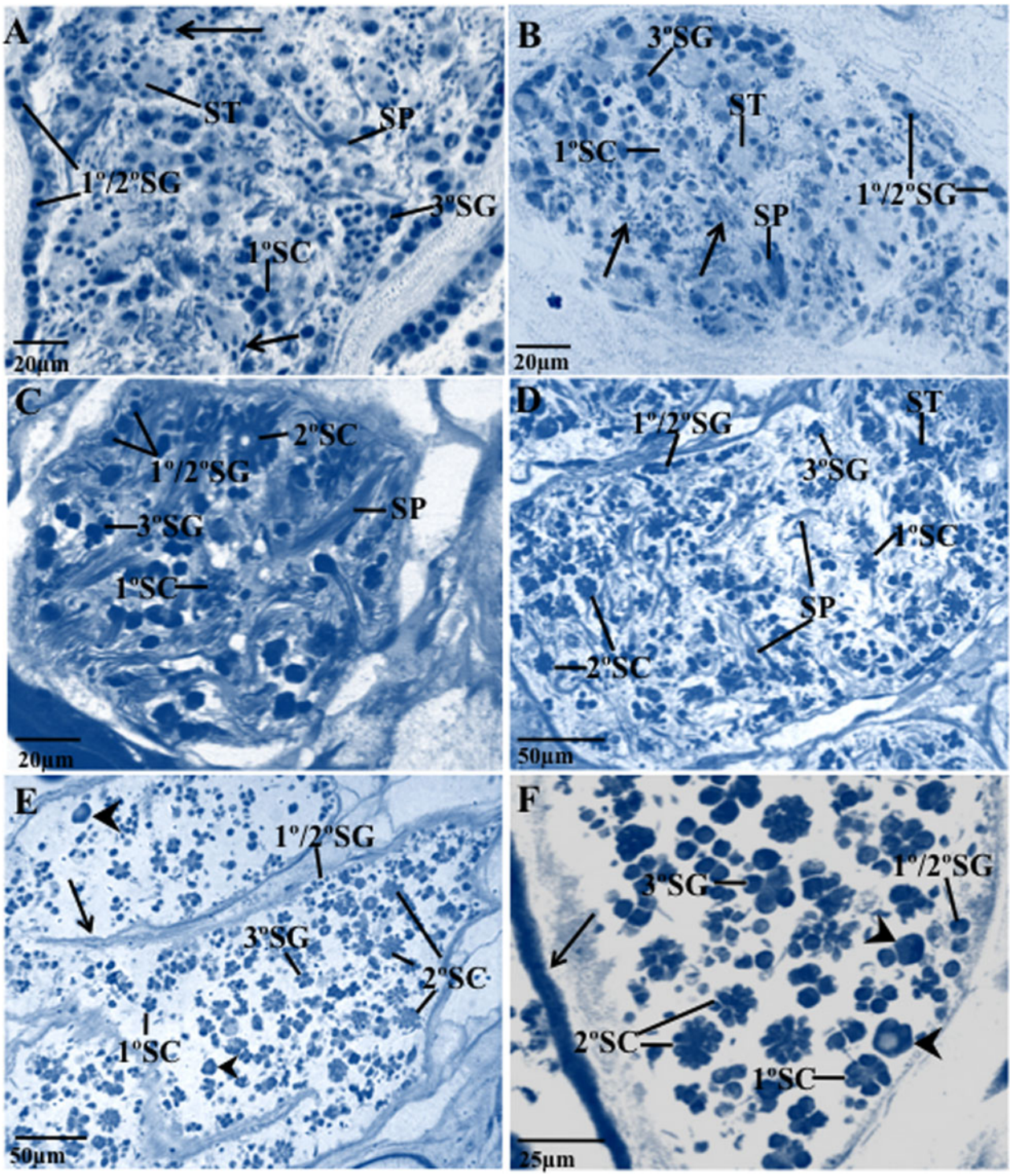

Fig. 1. Light micrographs of *Fasciola hepatica* (Sligo isolate) showing profiles of testis tubules of an untreated specimen (A); a fluke following *in vitro* treatment for 24 h with R(+)-verapamil (100 μM) (B); flukes following incubation *in vitro* for 15 h in TCBZ.SO (50 μg mL^{-1}) (C and D); and specimens treated *in vitro* with a combination of R(+)-verapamil (100 μM) + TCBZ.SO (50 μg mL^{-1}) until inactivity at 9 h (E and F). (A) Control fluke image. Primary (1°SG) and secondary (2°SG) spermatogonia are located at the periphery of the testis tubule, and numerous tertiary (3°SG) spermatogonia are present. Few primary (1°SC) spermatocytes are evident. Spermatids (ST) are numerous, with evidence of nuclear elongation (arrows). SP, mature spermatozoa. (B) R(+)-verapamil-treated fluke. Testis tubule showing peripherally located primary (1°SG) and secondary (2°SG) spermatogonia, also tertiary (3°SG) spermatogonia. Spermatid clusters (ST) are present and spermatids at various stages of maturation and showing elongation of the nuclei (arrows) can also be seen. 1°SC, primary spermatocytes; SP, mature spermatozoa. (C) TCBZ.SO-treated fluke. Primary (1°SG) and secondary (2°SG) spermatogonia are located at the periphery of the tubule. Primary (1°SC) and secondary (2°SC) spermatocytes are more centrally located. Mature spermatozoa (SP) are present in close parallel bundles throughout the tubule. 3°SG, tertiary spermatogonia. (D) TCBZ.SO-treated fluke. Primary (1°SG) and secondary (2°SG) spermatogonia are present in close proximity to the peripheral wall. Tertiary spermatogonia (3°SG) are

https://doi.org/10.1017/S0031182014000377 Published online by Cambridge University Press

of the tubule (Fig. 2A). Primary spermatocytes retained a normal morphology, and synaptonemal complexes were present, indicating synapsis of meiosis at early prophase (Fig. 2B and C). Clusters of secondary spermatocyte cells were present, showing the typical reduction in the nucleo-cytoplasmic ratio, and the cells were connected via cytoplasmic bridges (Fig. 2D). The spermatid cells contained elongated nuclei with chromatin forming lamellar-like sheets. The accompanying zone of differentiation appeared normal, with a typical layer of microtubules beneath the plasma membrane (PM) (Fig. 2E). Sections of axonemes lying free in the lumen of the tubule showed that they possessed an arrangement of nine microtubules surrounding a single central element, which is typical of the spermatozoa in parasitic platyhelminths (Fig. 2F).

Treatment until inactivity at 15 h with TCBZ.SO (50 μg mL^{-1})

The spermatogonia located beneath the peripheral wall of the tubule appeared normal and showed a typically high nucleo-cytoplasmic ratio (Fig. 3A). Primary spermatocytes were present in the tubule and mitochondria appeared to be congregated at the edge of the cell cluster (Fig. 3B). Secondary spermatocytes were typically located at the centre of the tubule and numerous cytoplasmic bridges connecting the cells were visible (Fig. 3C). Differentiation of the spermatid cells was evident, the cells containing elongated nuclei which were located at the periphery of the cell mass and whose content appeared to be condensed. However, in some regions the nuclei were clustered together and spermatid elongation was disrupted. The mitochondria appeared normal and were congregated at the edge of the spermatid cell cluster (Fig. 3D). Mature spermatozoa were abundant within the tubule (Fig. 3D–F). Cross-sections of the mature spermatozoa showed that the nucleus and axonemes were present, but that mitochondria were not visible (Fig. 3E). In a different region of the tubule, the axonemes and cortical microtubules were evident in the mature spermatozoa, but their mitochondria were disrupted (Fig. 3F).

Treatment until inactivity at 9 h with a combination of TCBZ.SO (50 μg mL^{-1}) and R(+)-VPL (100 μM)

Disruption was observed at all stages of spermatogenesis and discrete cell stages were often difficult to distinguish. The number of primary and secondary spermatogonia close to the peripheral wall of the tubule was low and disruption was evident to the nuclear and cell membranes. The membranes had little definition and the cell membrane was ruptured in places (Fig. 4A). The breakdown of the nuclear membrane and of the chromatin within the nucleus suggest that the cells were undergoing karyorrhexis. The primary spermatocytes were irregular in appearance, with disrupted nuclei, which were misshapen and the chromatin clumped, exemplifying pyknosis. The cell membrane of a primary spermatocyte was ruptured in one region. Electron-lucent areas were present in the cytoplasm and the mitochondria were swollen (Fig. 4B). Spermatid development appeared to be disrupted, in that the chromatin in the nucleus was loosely arranged into lamellar-like sheets, but elongation of the cell body was not apparent. Formation of the zone of differentiation was observed, which was separated from the main body of the spermatid cluster by a distinct collar (Fig. 4C). Axonemes were visible and seen to be extending away from the basal bodies in this zone (Fig. 4C). Late spermatid development was evident in the tubule. Within the median processes of the developing spermatozoa, the arrangement of microtubules appeared to be normal, although patches of electron-lucent material were present, suggesting possible nuclear or mitochondrial breakdown. The median processes and the axonemes appeared to be distinct from each other (Fig. 4D). Mature spermatozoa were severely disrupted throughout the follicle. The normal doublet arrangement of axonemes within a mature spermatozoon was not the general rule, but rather the presence of multi-axonemal structures, which were widespread throughout the follicle; these multi-axonemal structures often contained electron-lucent mitochondria and nuclei with a very granular appearance (Fig. 4E). In some regions of the tubule, mature spermatozoa appeared to be extensively swollen, with electron-lucent nuclei, although the axonemes within the spermatozoa appeared to have the normal '9 + 1' arrangement of microtubules.

numerous and located in the central tubule region. Mature spermatozoa (SP) are also numerous and are located throughout the tubule. 1°SC, primary spermatocytes; 2°SC, secondary spermatocytes. (E) Combination-treated fluke. Few primary (1°SG) and secondary (2°SG) spermatogonia are visible along the tubule wall (arrow) and only a small number of tertiary spermatogonia (3°SG) can be seen. Large apoptotic-like bodies can be seen in the tubule (arrowheads). No mature spermatozoa were visible in the tubule. 1°SC, primary spermatocytes; 2°SC, secondary spermatocytes. (F) Combination-treated fluke. Few primary (1°SG) and secondary (2°SG) spermatogonia are visible along the tubule wall (arrow). Tertiary (3°SG) spermatogonia are present in the central region of the tubule. Primary (1°SC) and secondary (2°SC) spermatocytes are present, but no mature spermatozoa or spermatids are visible. Large apoptotic-like bodies are present in the tubule (arrowheads).

https://doi.org/10.1017/S0031182014000377 Published online by Cambridge University Press

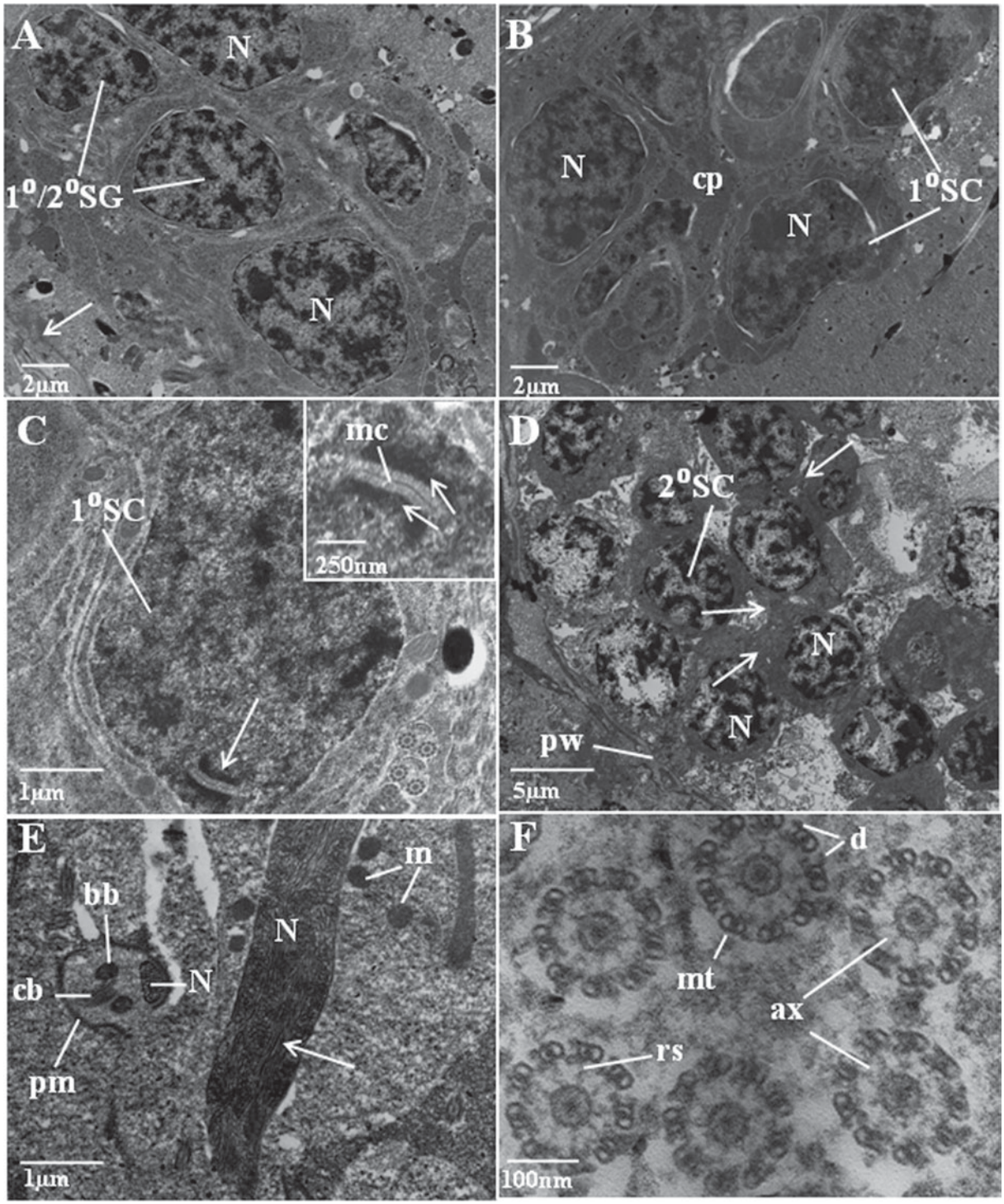

Fig. 2. Transmission electron micrographs (TEMs) showing profiles of testis tubules of *Fasciola hepatica* (Sligo isolate) following *in vitro* treatment for 24 h with R(+)-verapamil (100 μM). (A) A TEM showing a group of spermatogonia (1°/2°SG) in close proximity to the wall (arrowed) of the testis tubule. N, nucleus. (B) A TEM of a group of primary spermatocytes (1°SC), which are joined together by the central cytophore (cp). N, nucleus. (C) TEM of the nucleus of an individual primary spermatocyte (1°SC) containing a visible synaptonemal complex (arrow). Inset shows a high magnification image of the synaptonemal complex, which consists of two homologous chromosomes separated by a medial complex (mc) and with heterochromatin (arrows) visible on either side of the complex. (D) A TEM showing a cluster of secondary spermatocyte (2°SC) cells, with cytoplasmic bridges (arrows) connecting the cells. Pw, peripheral wall of the tubule; N, nucleus. (E) A TEM of a spermatid cell showing the elongation of the nucleus (N), and the chromatin within the nucleus which is organized into lamellar-like sheets (arrow). Basal bodies (bb), a central body (cb) and mitochondria (m) are also evident. A single row of peripheral microtubules lies beneath the plasma membrane (PM). (F) A TEM of a cross-section of six axonemes (ax), each possessing 9 sets of outer doublet microtubules (mt) arranged around a central element. Dynein side-arms (d) are visible on the outer microtubules, and radial spokes (rs) connect the microtubules to the central element.

https://doi.org/10.1017/S0031182014000377 Published online by Cambridge University Press

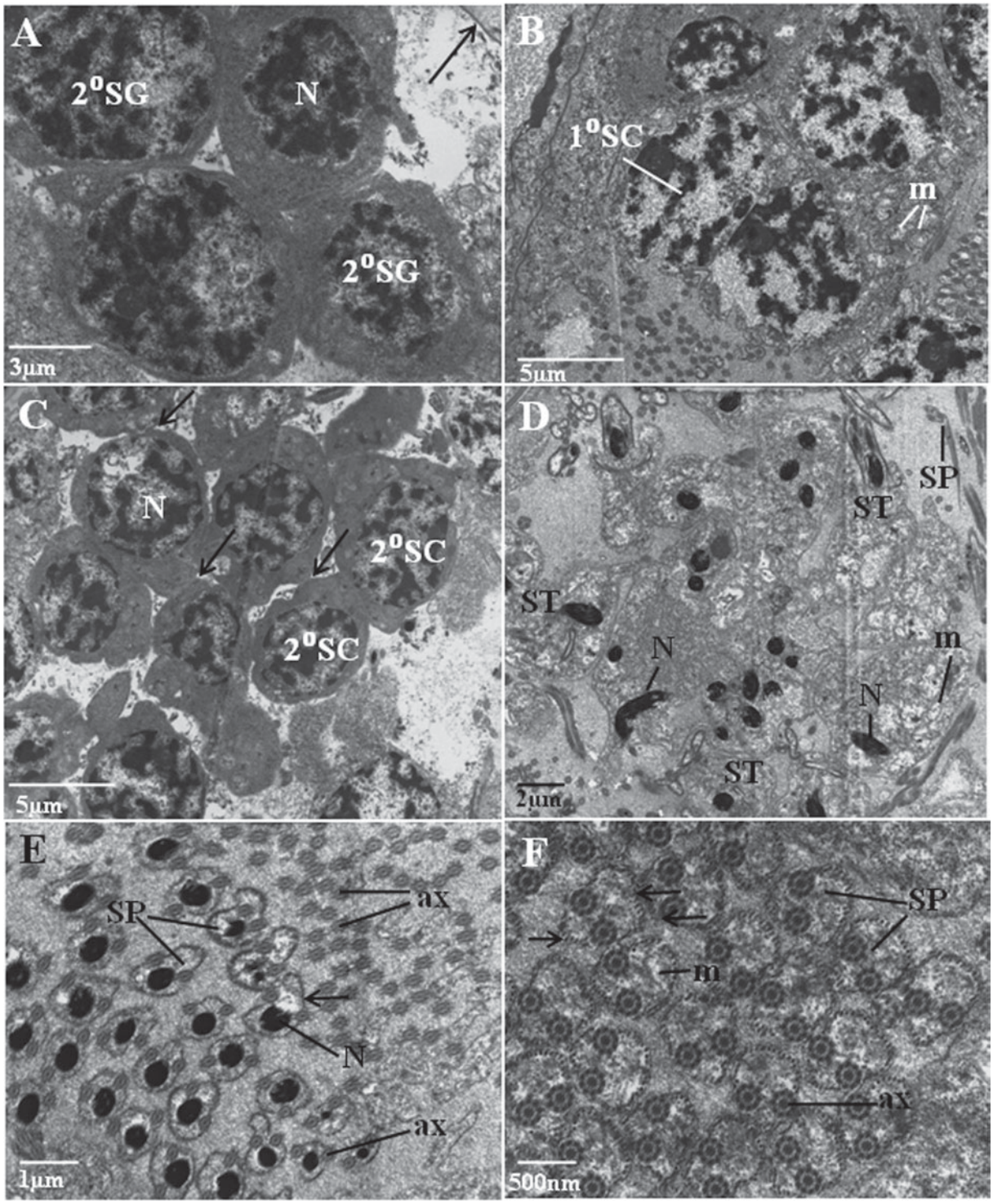

Fig. 3. Transmission electron micrographs (TEMs) showing profiles of testis tubules of *Fasciola hepatica* (Sligo isolate) following *in vitro* treatment with TCBZ.SO (50 μg mL^{-1}) until inactivity at 15 h. (A) TEM of a group of secondary spermatogonia (2°SG) located near to the wall (arrow) of the testis tubule, showing the typically high nucleocytoplasmic ratio. N, nucleus. (B) TEM showing a group of primary spermatocytes (1°SC). Mitochondria (m) are present in the cytoplasm of the cells at the edge of the cell cluster and appear to be normal. (C) TEM showing a cluster of secondary spermatocyte (2°SC) cells, with numerous cytoplasmic bridges (arrows) connecting them. N, nucleus. (D) TEM showing a section through a rosette of spermatid (ST) cells. Elongated nuclei (N) are visible and elongation of individual spermatid cells has occurred. Mature spermatozoa (SP) are visible at the edge of the spermatid rosette. The mitochondria (m) appear normal. (E) TEM showing transverse sections of mature spermatozoa (SP), containing nuclei (N), axonemes (ax) and cortical microtubules (arrow). Free axonemes are also visible in the lumen of the tubule. (F) TEM showing transverse sections of mature spermatozoa (SP). Axonemes (ax) and cortical microtubules (arrows) are visible within the spermatozoa. The mitochondria (m) in the spermatozoa appear to be disrupted and no nuclei are visible.

https://doi.org/10.1017/S0031182014000377 Published online by Cambridge University Press

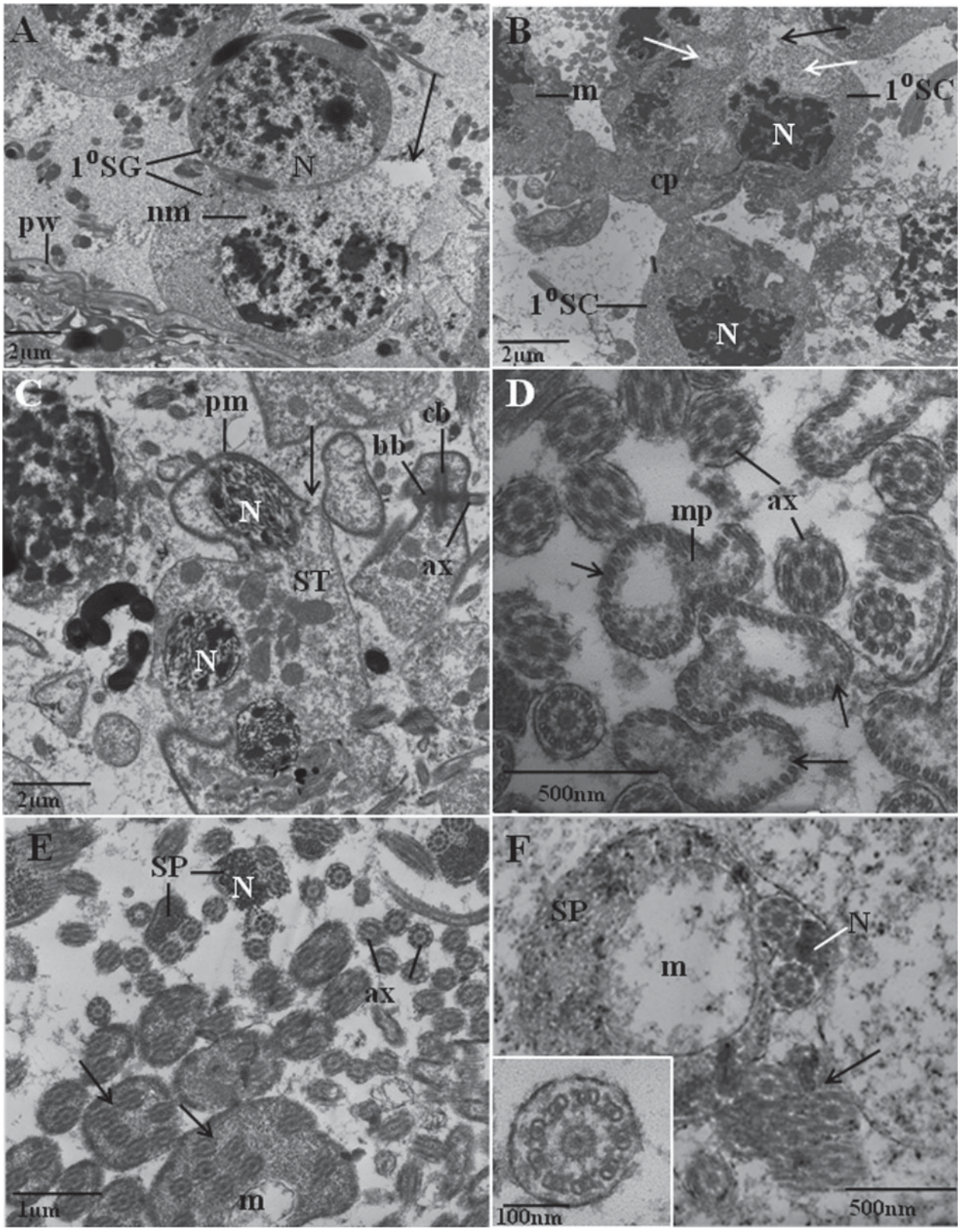

Fig. 4. Transmission electron micrographs (TEMs) showing profiles of testis tubules of *Fasciola hepatica* (Sligo isolate) following *in vitro* treatment with a combination of R(+)-verapamil (100 μM) + TCBZ.SO (50 μg mL^{-1}) until inactivity at 9 h. (A) TEM showing a cross-section of two primary spermatogonial (1°SG) cells in close proximity to the peripheral wall (pw) of the testis tubule. Disruption to the nucleus (N) is evident, with loss of definition of the nuclear membrane (nm). The cell membrane has ruptured (arrow) and the cytoplasm is electron-lucent in this region. (B) TEM showing a cluster of primary spermatocytes (1°SC) containing irregular nuclei (N) with dense chromatin. The cell membrane appears to have ruptured (black arrow) in one region, and large electron-lucent areas (white arrows) are present within the cytoplasm. The mitochondria (m) appear rounded and swollen. Cp, cytophore. (C) TEM of a cross-section of

https://doi.org/10.1017/S0031182014000377 Published online by Cambridge University Press

The mitochondria were abnormally large and electron-lucent. The nucleus of the spermatozoon was visible between the two axonemes and appeared to be irregular in shape (Fig. 4F). A multi-axonemal structure was observed in close proximity to the mature spermatozoon (Fig. 4F).

Vitelline ultrastructure

The ultrastructure of the vitellaria in the 24 h control specimens was normal (and similar to the 0 h controls), as described by Irwin and Threadgold (1970) and Colhoun *et al*. (1998). Thus, no abnormalities were noted following incubation *in vitro*.

Treatment for 24 h with R(+)-VPL (100 μM)

The morphology of the vitelline follicles appeared to be normal after treatment, as they contained a normal heterogeneous population of stem cells, nurse cells, intermediate type 1 (It1) and type 2 (It2) cells and mature cells. Nurse cells and stem cells were present at the periphery of the follicle, whilst mature stages were more centrally located within the follicle (Fig. 5A and B).

Treatment until inactivity at 15 h with TCBZ.SO (50 μg mL^{-1})

The morphology of the vitelline follicle had changed slightly after treatment. Swelling of the cisternae of the granular endoplasmic reticulum was evident in the It2 cells and large single shell protein globules were present. The stem cells appeared normal (Fig. 5C). The mature vitelline cells contained glycogen deposits, yolk globules and small shell globule clusters, which appeared normal, although the cisternae of the granular endoplasmic reticulum were swollen (Fig. 5D). The organization of the vitelline follicles generally appeared normal, with mature cells located in the central region, whilst nurse cells, stem cells and It1 and It2 cells were located more peripherally within the follicle (Fig. 5E). Only small, single shell protein globules were present in It1 cells (Fig. 5E) In some instances, the organization of cells in the follicle appeared abnormal, as nurse cells and It1 cells were unusually located in the centre of the follicle, with mature and It2 cells visible at the periphery of the follicle (Fig. 5F).

Treatment until inactivity at 9 h with a combination of TCBZ.SO (50 μg mL^{-1}) and R(+)-VPL (100 μM)

Following combination drug treatment, the vitelline follicles were disrupted at all stages of development. However, not all stages were obviously disrupted in all follicles, as differences in disruption were observed both between and within follicles in the same cell stages. Large spaces were evident between cells, due to the separation of cells from the nurse cell cytoplasm. Large single shell protein globules were present in It1 cells and swelling of the cisternae of the granular endoplasmic reticulum was evident. The It1 cells also appeared to have a rounded, rather than elongated, shape (Fig. 6A). Similar features were observed in It2 cells, with swelling of the cisternae of the granular endoplasmic reticulum and large single shell protein globules present. The stem cells were round in shape (Fig. 6B). The mature cells were often highly disrupted, with extensive cytoplasmic breakdown evident throughout the cell, although the shell protein globules appeared to be normal and the shell globule clusters remained tightly packed; the yolk globules also appeared to be normal (Fig. 6C). Extreme swelling of the cisternae of the granular endoplasmic reticulum was evident in some It2 cells, although It1 cells in the same follicle appeared undisrupted. Large single shell protein globules were present in the It2 cells (Fig. 6D). There appeared to be relatively more It2 and mature cells in the follicles than usual.

Note

The changes seen in the spermatogenic and vitelline cells following the various treatments were consistent between specimens.

an abnormal cluster of spermatid (ST) cells. The chromatin within the nucleus (N) appears to be loosely arranged into lamellar-like sheets, but elongation of the nucleus is not evident. The plasma membrane (pm) appears thickened and invaginated to form a groove-like collar (arrow). The zone of differentiation of a spermatid cell is visible, with one axoneme (ax) extending away from its basal body (bb); the two basal bodies are situated on either side of the central body (cb). (D) TEM showing a cross-section through the median process (mp) and axonemes (ax) which are separate from one another. The median process (mp) is lined with cortical microtubules (arrows). The centre of the median process appears to be very electron-lucent. A large number of free axonemes is present in close proximity to the median processes. (E) TEM showing a cluster of spermatozoa in various abnormal states. Multi-axonemal spermatozoa (arrows) are present, some of which contain disrupted, electron-lucent mitochondria (m). Multiple free axonemes (ax) are also visible. Other spermatozoa (SP) contain a nucleus (N) which is irregular in shape and its content is abnormally granular. (F) A cross-section of a mature spermatozoon (SP) which appears to be extremely swollen and contains an abnormally large electron-lucent mitochondrion (m). A multi-axonemal spermatozoon (arrow) is also present. Inset shows a high-power micrograph of an individual axoneme, which possesses the normal 9 + 1 arrangement of microtubules. N, nucleus.

https://doi.org/10.1017/S0031182014000377 Published online by Cambridge University Press

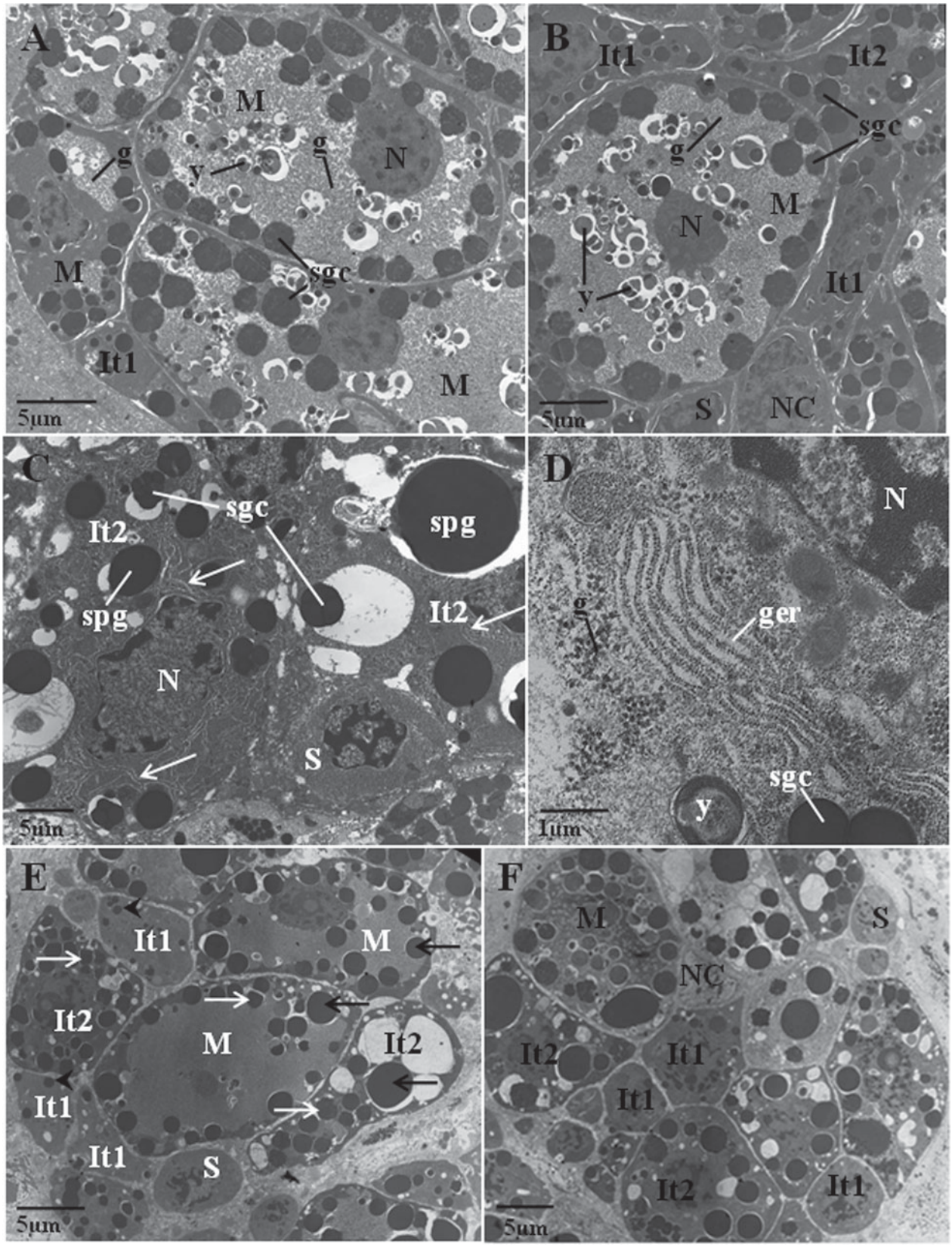

Fig. 5. Transmission electron micrographs (TEMs) showing the vitelline follicles of *Fasciola hepatica* (Sligo isolate) following *in vitro* treatment with R(+)-verapamil (100 μM) for 24 h (A and B), and TCBZ.SO (50 μg mL^{-1}) until inactivity at 15 h (C-F). (A) R(+)-verapamil-treated fluke. A low-power TEM of a vitelline follicle containing mature vitelline cells (M) and an intermediate type 1 cell (It1). Shell globule clusters (sgc), glycogen (g) and yolk globules (y) are present in the mature cells, and eggshell globule clusters are present in the It1 cell. N, nucleus. (B) R(+)-verapamil-treated fluke. A TEM showing a vitelline follicle containing all stages of cell development. A mature cell (M) and a number of intermediate type 1 (It1) and type 2 (It2) vitelline cells are present, along with a stem cell (S) and a nurse cell

https://doi.org/10.1017/S0031182014000377 Published online by Cambridge University Press

DISCUSSION

From the results of this investigation, it is evident that co-incubation of TCBZ.SO with the Pgp inhibitor, R(+)-VPL greatly increases the impact of TCBZ.SO on the reproductive tissues of the TCBZ-R Sligo isolate of *F. hepatica*. The combination also reduced the time taken for flukes to cease movement (Savage *et al*. 2013*a*). The implications of the results for the mechanism of resistance to TCBZ and on the reproductive output potential of the fluke will be discussed below.

Taking the testis first, incubation in R(+)-VPL alone did not alter the morphology or relative numbers of spermatogenic cells. Treatment with TCBZ.SO on its own induced few changes to the cells and no diminution of the cell population within the tubule. Sperm formation continued, although on occasion spermatid elongation was affected, as were the mitochondria within the spermatozoa. However, there was a sharp drop in the number of cells in the testis tubule following co-incubation in TCBZ.SO + R(+)-VPL, with few spermatogonia and apoptotic spermatocytes; the latter are equivalent to the eosinophilic, multinucleate cells initially identified by Hanna *et al*. (2008) and also described by Hanna *et al*. (2010, 2012*a*, 2013), McConville *et al*. (2010), Scarcella *et al*. (2011) and Toner *et al*. (2011*b*). What spermatids and spermatozoa were present were abnormal. Typically, the sperm were multiaxonemal, often swollen and their nuclei and mitochondria were electron-lucent.

The block in mitotic division of the spermatogenic cells and formation of aberrant sperm are changes typical of microtubule inhibition and compatible with the presumed anti-microtubule action of TCBZ. Similar changes have been observed in TCBZ-S flukes following incubation in TCBZ.SO *in vitro* (Stitt and Fairweather, 1992) and following treatment with TCBZ *in vivo* (Toner *et al*. 2011*b*). The changes have also been seen in experiments with microtubule inhibitors and the TCBZ analogue, compound alpha (Stitt and Fairweather, 1992; McConville *et al*. 2010). However, equivalent changes have not been seen in TCBZ-R flukes (Hanna *et al*. 2010, 2013). This suggests that Pgp inhibition has allowed the normal action of TCBZ to become apparent, leading to the apoptotic breakdown of the spermatogenic cells. Other flukicides and drugs induce different changes to the spermatogenic cells, a point discussed in more detail by McConville *et al*. (2010) and Toner *et al*. (2011*b*).

Turning to the vitellaria, incubation in R(+)-VPL on its own did not alter the morphology of the vitelline cells, the cell composition of the follicle or the overall ratio of different cell stages within the follicle. Few changes were seen after treatment with TCBZ.SO alone: e.g. a swelling of the cisternae of the granular endoplasmic reticulum and abnormal packaging of the shell protein globule. Far more severe changes were seen in the combination-treated flukes, involving all cell types and large spaces were evident between the cells. There was a shift in the cell population towards the later developmental stages and the mature cells were undergoing cytoplasmic breakdown.

The changes seen in the vitelline follicles of combination-treated TCBZ-R flukes were similar to those evident following treatment of TCBZ-S isolates with TCBZ.SO *in vitro* (Stitt and Fairweather, 1996) and TCBZ *in vivo* (Toner *et al*. 2011*a*). They are representative of microtubule disruption and, as with the changes in the testis, the drug sensitivity of the Sligo isolate has been changed to a more susceptible state by co-incubation with a Pgp inhibitor. Other drugs induce different changes to the vitellaria (Fairweather *et al*. 1988; Skuce and Fairweather, 1988; Stitt and Fairweather, 1991; Colhoun *et al*. 1998; Toner *et al*. 2008; Halferty *et al*. 2009). So, the changes seen in the current study with respect to the testis and vitellaria are specific to TCBZ.SO and do not simply represent a general response to any drug. It is known that disruption of the vitelline cells and spermatozoa following TCBZ treatment *in vivo* leads to abnormalities in egg formation, culminating in the complete cessation of egg production (Hanna *et al*. 2010, 2012*a*; Toner *et al*. 2011*a*). So, the changes seen in the two tissues following R(+)-VPL co-treatment with TCBZ.SO would have a serious impact on the reproductive

(NC). Shell globule clusters (sgc), glycogen granules (g), a nucleus (N) and yolk globules (y) are all visible in the mature cell. Shell globule clusters are also present in the It1 and It2 cells. (C) TCBZ.SO-treated fluke. A TEM showing intermediate type 2 (It2) vitelline cells containing large single shell protein globules (spg) and small shell globule clusters (sgc). Swelling (arrows) of the cisternae of granular endoplasmic reticulum is evident in the It2 cells. S, stem cell. (D) TCBZ.SO-treated fluke. A high-power TEM showing swelling of the cisternae of granular endoplasmic reticulum (ger) in a mature vitelline cell. A shell globule cluster (sgc) is present, as are glycogen granules (g) and yolk globules (y). N, nucleus. (E) TCBZ.SO-treated fluke. A TEM of a vitelline follicle containing mature cells (M) at the centre of the follicle, and intermediate type 1 (It1) and type 2 (It2) cells and a stem cell (S) at the periphery of the follicle. Large shell protein globules (black arrows) and small shell globule clusters (white arrows) are present in mature and It2 cells, while only small, single shell protein globules (arrowheads) are present in It1 cells. (F) TCBZ.SO-treated fluke. A low-power TEM showing an abnormal distribution of cells within a vitelline follicle. A nurse cell (NC) and It1 (It1) cells are situated in the centre of the follicle, whilst It2 (It2) and mature (M) cells are situated at the periphery. S, stem cell.

https://doi.org/10.1017/S0031182014000377 Published online by Cambridge University Press

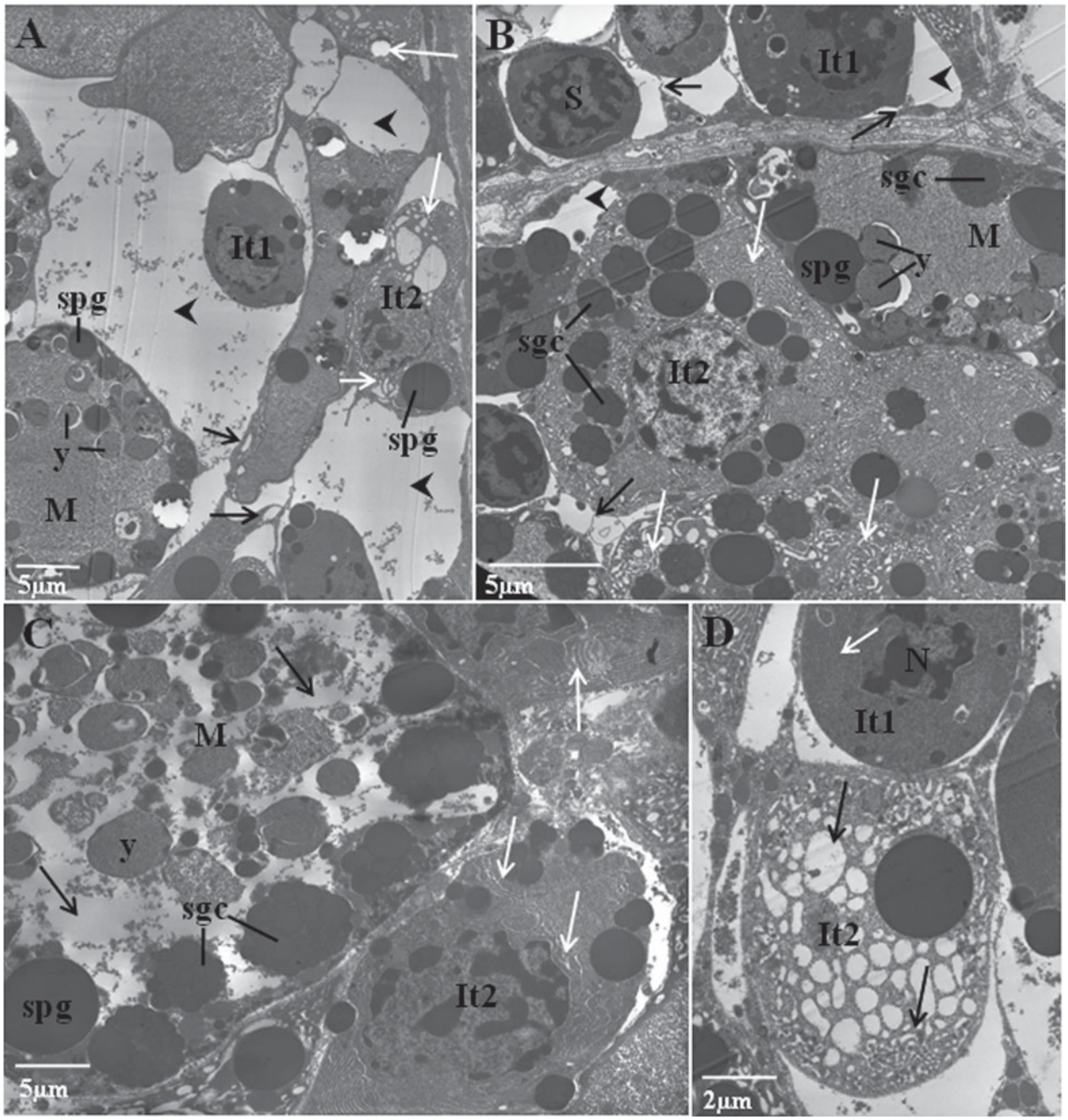

Fig. 6. Transmission electron micrographs (TEMs) showing the vitelline follicles of *Fasciola hepatica* (Sligo isolate) following *in vitro* treatment with a combination of R(+)-verapamil (100 μM) + TCBZ.SO (50 μg mL^{-1}) until inactivity at 9 h. (A) TEM showing separation of the vitelline cells from the nurse cell processes (black arrows) which has resulted in large open spaces (arrowheads) within the follicle. Intermediate type 1 (It1) cells appear rounded and swelling of the cisternae of granular endoplasmic reticulum (white arrows) is evident within the It2 (It2) cell. Yolk globules (y) and shell protein globules (spg) are present within the mature cell (M). (B) A TEM showing separation of the vitelline cells from the nurse cell processes (black arrows) which has resulted in large open spaces (arrowheads) between the vitelline cells. Swelling of the cisternae of granular endoplasmic reticulum (white arrows) is visible in an intermediate type 2 (It2) cell. Large shell protein globules (spg) and shell globule clusters (sgc) are present in the mature (M) and It2 cells. It1, intermediate type 1 cell; S, stem cell; y, yolk globules. (C) TEM showing breakdown of the cytoplasm (black arrows) within a mature vitelline cell (M). Shell protein globules (spg), shell globule clusters (sgc) and yolk globules (y) remain intact. Slight swelling of the cisternae of the granular endoplasmic reticulum (white arrows) can be seen in intermediate type 2 (It2) cells. (D) A high-power TEM showing discrete differences in disruption within intermediate-type vitelline cells. There is extreme swelling of the cisternae of granular endoplasmic reticulum (arrows) in the It2 (It2) cell, whilst the granular endoplasmic reticulum appears normal in the adjacent It1 (It1) cell. N, nucleus.

https://doi.org/10.1017/S0031182014000377 Published online by Cambridge University Press

capacity of TCBZ-R flukes. Knockdown of the SMDR2 and SmMRP1 transporter genes in *Schistosoma mansoni* has been shown to cause a reduction in egg production (Kasinathan *et al*. 2011). In the same study, incubation of worms *in vitro* with R(+)-VPL alone led to a drop in egg production; this was attributed to a disruption of oocyte development in the ovary. Whilst the ovary was not examined in the present study on *F. hepatica*, it is interesting that R(+)-VPL alone had no effect on the testis or vitelline follicle. Egg hatch data have shown that eggs of TCBZ-R fluke isolates are more resistant to the action of TCBZ than those of TCBZ-S isolates (Fairweather *et al*. 2012). Pgp has been localized in the multi-layered eggshell of nematode parasites and the level of staining is greater in anthelmintic-resistant than -susceptible isolates (Kerboeuf *et al*. 1999, 2003*b*; Riou *et al*. 2005). It was suggested that the role of Pgp in the eggshell is to protect the egg from the toxic effects of xenobiotics such as anthelmintics. The eggshell of *F. hepatica* is a less complex structure, formed by the coalescence of shell protein material contained in the shell globule clusters in the vitelline cells, and it is possible that Pgp is associated with these clusters.

The existence of large spaces between the cells within the vitelline follicle indicates that the nurse cell network has been disrupted. As well as providing a support(ing) framework for the cells, the nurse cells serve to transfer precursor molecules from the parenchyma to the vitelline cells, which is essential for their development (Irwin and Threadgold, 1970). The loss of contact between the cells and the nurse cell processes prevents that exchange and supply of nutrients to the cells from taking place. A similar network exists in the testis tubules, emanating from the sustentacular cells, and these cells have a similar function to the nurse cells (Hanna *et al*. 2012*b*). The sustentacular cells are analogous to the Sertoli cells in the mammalian testis, which support, protect and nourish the germ cells (Griswold and McLean, 2006). The Sertoli cells express a diverse array of drug transporters, including Pgp, which serve to protect the germ cells from the harmful effects of xenobiotics by preventing their entry into the testis (Melaine *et al*. 2002; Su *et al*. 2011; Robillard *et al*. 2012). Disruption to the sustentacular tissue following TCBZ treatment *in vivo* has been described by Toner *et al*. (2011*b*). Pgp has been located in the cytoplasmic networks within the vitelline follicles and testis tubules of *F. hepatica* (Wells, 2008). It is possible that Pgp-linked efflux pumps are involved in the exchange of materials between the parenchyma and the cells within these two organs. The level of Pgp activity in TCBZ-S flukes may not be sufficient to protect the vitelline and spermatogenic cells from the effects of TCBZ. In TCBZ-R flukes, however, a greater expression of Pgp would normally shield the cells, but inhibition by R(+)-VPL would allow TCBZ to gain access to the cells, leading to the disruption seen.

The changes to the vitelline and spermatogenic cells induced by the drug combination occurred very quickly *in vitro* (after only 9 h incubation). They are consistent with the changes to the tegument and gut described previously (Savage *et al*. 2013*a*, *b*). Translating the morphological disruption and inactivity data to the *in vivo* situation, they would undoubtedly hasten the 'death' and elimination of the fluke and lead to greater efficacy of TCBZ against TCBZ-R flukes. Enhanced efficacy of anthelmintic + VPL combinations against nematode parasites has been demonstrated by Molento and Prichard (1999), Bartley *et al*. (2009, 2012) and Lifschitz *et al*. (2010*a*, *b*). Based on this evidence and data from other resistance reversal experiments carried out *in vitro*, the use of anthelmintics plus Pgp inhibitors has been proposed as a strategy to deal with drug resistance (e.g. Lespine *et al*. 2008, 2012; Kasinathan *et al*. 2010*a*, 2011; Lifschitz *et al*. 2010*a*, *b*; Kerboeuf and Riou, 2011; Kasinathan and Greenberg, 2012).

In conclusion, inhibition of Pgp activity in a TCBZ-R isolate of *F. hepatica* has altered (increased) the response of the testis and vitellaria to treatment with TCBZ.SO. That is, it has reversed the TCBZ-resistant phenotype of the fluke. The changes are representative of those normally seen in TCBZ-S flukes following exposure to TCBZ and are not simply non-specific drug-induced changes. Such potentiation of TCBZ activity may be due to the increased expression of Pgp-linked drug efflux pumps in TCBZ-R flukes, as previously suggested (Alvarez *et al*. 2005; Mottier *et al*. 2006), although this may not be the case (Fuchs *et al*. 2008). Alternatively, blocking of Pgp may simply increase the effective concentration of TCBZ/TCBZ.SO within the fluke, thereby overcoming a separate mechanism of resistance (see below). It is known that TCBZ-R flukes possess a variant allele for Pgp (Wilkinson *et al*. 2012); this may be more efficient at pumping out TCBZ metabolites. The results support other morphological, pharmacological and molecular data for the role of Pgp in resistance to TCBZ, as referred to in the Introduction. The same mechanism appears to be displayed by TCBZ-R fluke isolates from three different countries (Australia, Ireland and the Netherlands), suggesting that it has arisen independently in each case. It may not be the only resistance mechanism in operation, because greater drug metabolizing activity has been demonstrated in both the Sligo isolate (Robinson *et al*. 2004; Alvarez *et al*. 2005) and the Oberon isolate. In the case of the latter, drug sensitivity can be reversed by the use of inhibitors of detoxifying enzyme pathways (e.g. Devine *et al*. 2011, 2012). These two non-specific mechanisms seem to be more important than any specific changes in the presumed target molecule

https://doi.org/10.1017/S0031182014000377 Published online by Cambridge University Press

for TCBZ, namely, *β*-tubulin (Ryan *et al*. 2008). Their combined effect would serve to block TCBZ and its metabolites from reaching their target. While the present results point towards a role for drug transporters in resistance to TCBZ, more needs to learnt about their identity and localization in *F. hepatica*, their expression in TCBZ-S and -R isolates and the interaction between the transporters and Pgp inhibitors. Future work could also involve the use of other Pgp inhibitors, to confirm the phenomenon, and application of some form of statistical analysis to the morphological data. As far as the authors are aware, the latter has not been attempted in other drug studies on *F. hepatica* (or other helminth parasites). Semi-quantitative analyses have been carried out (e.g. Hanna *et al*. 2010, 2013; Devine *et al*. 2011, 2012; Meaney *et al*. 2013; Savage *et al*. 2013*a*); they might have been useful in underpinning the results, although in this case the differences in responses between drug treatments were clear-cut.

ACKNOWLEDGEMENTS

This work was supported by a DARDNI Postgraduate Studentship to Joanne Savage. It was also partially supported by a grant from the European Union (DELIVER grant, no. FOOD-CT-200x-023025) and by a BBSRC/Defra grant (C00082X/1).

REFERENCES

Alvarez, L. I., Solana, H. D., Mottier, M. L., Virkel, G. L., Fairweather, I. and Lanusse, C. E. (2005). Altered drug influx/efflux and enhanced metabolic activity in triclabendazole resistant liver flukes. *Parasitology* **131**, 501–510.

Bartley, D. J., McAllister, H., Bartley, Y., Dupuy, J., Menez, C., Alvinerie, M., Jackson, F. and Lespine, A. (2009). P-glycoprotein interfering agents potentiate ivermectin susceptibility in ivermectin sensitive and resistant isolates of *Teladorsagia circumcinta* and *Haemonchus contortus*. *Parasitology* **136**, 1081–1088.

Bartley, D. J., Morrison, A. A., Dupuy, J., Bartley, Y., Sutra, J. F., Menez, C., Alvineire, M., Jackson, F., Devin, L. and Lespine, A. (2012). Influence of Pluronic 85 and ketoconazole on disposition and efficacy of ivermectin in sheep infected with a multiple resistant *Haemonchus contortus* isolate. *Veterinary Parasitology* **187**, 464–472.

Biscardi, M., Teodori, E., Caporale, R., Budriesi, R., Balestri, F., Scappini, B., Gavazzi, S. and Grossi, A. (2006). Multidrug reverting activity toward leukemia cells in a group of new verapamil analogues with low cardiovascular activity. *Leukemia Research* **30**, 1–8.

Choi, S. U., Lee, C. O., Kim, K. H., Choi, E. J., Park, S. H., Shin, H. S., Yoo, S. E., Jung, N. P. and Lee, B. H. (1998). Reversal of multidrug resistance by novel verapamil analogs in cancer cells. *Anti-Cancer Drugs* **9**, 157–165.

Colhoun, L. M., Fairweather, I. and Brennan, G. P. (1998). Observations on the mechanism of eggshell formation in the liver fluke, *Fasciola hepatica*. *Parasitology* **116**, 555–567.

Devine, C., Brennan, G. P., Lanusse, C. E., Alvarez, L. I., Trudgett, A., Hoey, E. M. and Fairweather, I. (2011). Enhancement of triclabendazole action *in vivo* against a triclabendazole-resistant isolate of *Fasciola hepatica* by co-treatment with ketoconazole. *Veterinary Parasitology* **177**, 305–315.

Devine, C., Brennan, G. P., Lanusse, C. E., Alvarez, L. I., Trudgett, A., Hoey, E. and Fairweather, I. (2012). Potentiation of triclabendazole action *in vivo* against a triclabendazole-resistant isolate of *Fasciola hepatica* following its co-administration with the metabolic inhibitor, ketoconazole. *Veterinary Parasitology* **184**, 37–47.

Echizen, H., Brecht, T., Niedergesass, S., Vogelgesang, B. and Eichelbaum, M. (1985). The effect of dextro-, levo-, and racemic verapamil on atrioventricular conduction in humans. *American Heart Journal* **109**, 210–217.

Fairweather, I. (2011). Liver fluke isolates: a question of provenance. *Veterinary Parasitology* **176**, 1–8.

Fairweather, I., Anderson, H. R. and Threadgold, L. T. (1988). *Fasciola hepatica*: morphological changes in vitelline cells following treatment *in vitro* with the deacetylated (amine) metabolite of diamphenethide (DAMD). *International Journal for Parasitology* **18**, 1061–1069.

Fairweather, I., McShane, D. D., Shaw, L., Ellison, S. E., O'Hagan, N. T., York, E. A., Trudgett, A. and Brennan, G. P. (2012). Development of an *in vitro* egg hatch assay for the diagnosis of triclabendazole resistance in *Fasciola hepatica*: proof of concept. *Veterinary Parasitology* **183**, 249–259.

Fuchs, M., Ryan, L., Brennan, G., Trudgett, A., Fairweather, I. and Hoey, E. (2008). Triclabendazole resistance in the liver fluke, *Fasciola hepatica*: scanning candidate genes for mutations and mRNA-expression levels. In *Proceedings of the Tenth European Multicolloquium of Parasitology* (EMOP X), Paris, France, abstract no. SY04/0605, p. 49.

Griswold, M. D. and McLean, D. (2006). The sertoli cell. In *Knobil and Neill's Physiology of Reproduction* (ed. Neill, J. D.), pp. 949–975. Academic Press, London, UK.

Halferty, L., O'Neill, J. F., Brennan, G. P., Keiser, J. and Fairweather, I. (2009). Electron microscopical study to assess the *in vitro* effects of the synthetic trioxolane OZ78 against the liver fluke, *Fasciola hepatica*. *Parasitology* **136**, 1325–1337.

Hanna, R. E. B., Edgar, H., Moffett, D., McConnell, S., Fairweather, I., Brennan, G. P., Trudgett, A., Hoey, E. M., Cromie, L., Taylor, S. M. and Daniel, R. (2008). *Fasciola hepatica*: histology of the testis in egg-laying adults of several laboratory-maintained isolates of flukes grown to maturity in cattle and sheep and in flukes from naturally infected hosts. *Veterinary Parasitology* **157**, 222–234.

Hanna, R. E. B., Edgar, H. W. J., McConnell, S., Toner, E., McConville, M., Brennan, G. P., Devine, C., Flanagan, A., Halferty, L., Meaney, M., Shaw, L., Moffett, D., McCoy, M. and Fairweather, I. (2010). *Fasciola hepatica*: histological changes in the reproductive structures of triclabendazole (TCBZ)-sensitive and TCBZ-resistant flukes after treatment *in vivo* with TCBZ and the related benzimidazole derivative, compound alpha. *Veterinary Parasitology* **168**, 240–254.

Hanna, R. E. B., Scarcella, S., Solana, H., McConnell, S. and Fairweather, I. (2012*a*). Early onset of changes to the reproductive system of *Fasciola hepatica* following *in vivo* treatment with triclabendazole. *Veterinary Parasitology* **184**, 341–347.

Hanna, R. E. B., Moffett, D., Brennan, G. P. and Fairweather, I. (2012*b*). *Fasciola hepatica*: a light and electron microscope study of sustentacular tissue and heterophagy in the testis. *Veterinary Parasitology* **187**, 168–182.

Hanna, R. E. B., Forster, F. I., Brennan, G. P. and Fairweather, I. (2013). *Fasciola hepatica*: histological demonstration of apoptosis in the reproductive organs of flukes of triclabendazole-sensitive and triclabendazole-resistant isolates, and in field-derived flukes from triclabendazole-treated hosts, using *in situ* hybridization to visualize endonuclease strand breaks. *Veterinary Parasitology* **191**, 240–251.

Höllt, V., Kouba, M., Dietel, M. and Vogt, G. (1992). Stereoisomers of calcium antagonists which differ markedly in their potencies as calcium blockers are equally effective in modulating drug transport by P-glycoprotein. *Biochemical Pharmacology* **43**, 2601–2608.

Holmes, S. D. (1983). *In vitro* studies into the mode of action of anthelmintics on the liver fluke, *Fasciola hepatica* L. Ph.D. thesis. The Queen's University of Belfast, Belfast, Northern Ireland.

Irwin, S. W. B. and Threadgold, L. T. (1970). Electron-microscope studies on *Fasciola hepatica* VIII. The development of the vitelline cells. *Experimental Parasitology* **28**, 399–411.

James, C. E., Hudson, A. L. and Davey, M. W. (2009). An update on P-glycoprotein and drug resistance in *Schistosoma mansoni*. *Trends in Parasitology* **25**, 538–539.

Kasinathan, R. S. and Greenberg, R. M. (2012). Pharmacology and potential physiological significance of schistosome multidrug resistance transporters. *Experimental Parasitology* **132**, 2–6.

Kasinathan, R. S., Goronga, T., Messerli, S. M., Webb, T. R. and Greenberg, R. M. (2010*a*). Modulation of a *Schistosoma mansoni* multi-drug transporter by the antischistosomal drug praziquantel. *FASEB Journal* **24**, 128–135.

Kasinathan, R. S., Morgan, W. M. and Greenberg, R. M. (2010*b*). *Schistosoma mansoni* express higher levels of multidrug resistance-associated protein 1 (SmMRP1) in juvenile worms and in response to praziquantel. *Molecular and Biochemical Parasitology* **173**, 25–31.

Kasinathan, R. S., Morgan, W. M. and Greenberg, R. M. (2011). Genetic knockdown and pharmacological inhibition of parasite multidrug resistance transporters disrupts egg production in *Schistosoma mansoni*. *PLoS Neglected Tropical Diseases* **5**, e1425.

Kerboeuf, D. and Riou, M. (2011). Efflux pump inhibitors: a progress in parasitic nematode control. *Bulletin de l'Académie Vétérinaire de France* **164**, 257–264.

Kerboeuf, D., Chambrier, P., Le Vern, Y. and Aycardi, J. (1999). Flow cytometry analysis of drug transport mechanisms in *Haemonchus contortus* susceptible or resistant to anthelmintics. *Parasitology Research* **85**, 118–123.

Kerboeuf, D., Blackhall, W., Kaminsky, R. and Von Samson-Himmelstjerna, G. (2003*a*). P-glycoprotein in helminths: function and perspectives for anthelmintic treatment and reversal of resistance. *International Journal of Antimicrobial Agents* **22**, 332–346.

Kerboeuf, D., Guénard, F. and Le Vern, Y. (2003*b*). Detection of P-glycoprotein-mediated multidrug resistance against anthelmintics in *Haemonchus contortus* using anti-human mdr1 monoclonal antibodies. *Parasitology Research* **91**, 79–85.

Kumar, V., Abbas, A. K. and Fausto, N. (2005). Cellular responses to stress and toxic insults: adaptation, injury and death. In *Robbins and Cotran Pathologic Basis of Disease*, 7th Edn, pp. 26–32. Elsevier Saunders, Philadelphia, PA, USA.

Lespine, A., Alvinerie, M., Vercruysse, J., Prichard, R. K. and Geldhof, P. (2008). ABC transporter modulation: a strategy to enhance the activity of macrocyclic lactone anthelmintics. *Trends in Parasitology* **24**, 293–298.

Lespine, A., Ménez, C., Bourguinat, C. and Prichard, R. K. (2012). P-glycoproteins and other multidrug resistance transporters in the pharmacology of anthelmintics: prospects for reversing transport-dependent anthelmintic resistance. *International Journal for Parasitology: Drugs and Drug Resistance* **2**, 58–75.

Lifschitz, A., Entrocasso, C., Alvarez, L., Lloberas, M., Ballent, M., Manazza, G., Virkel, G., Borda, B. and Lanusse, C. (2010*a*). Interference with P-glycoprotein improves ivermectin activity against adult resistant nematodes in sheep. *Veterinary Parasitology* **172**, 291–298.

Lifschitz, A., Suarez, V. H., Sallovitz, J., Cristel, S. L., Imperiale, F., Ahoussou, S., Schiavi, C. and Lanusse, C. (2010*b*). Cattle nematodes resistant to macrocyclic lactones: comparative effects of P-glycoprotein modulation on the efficacy and disposition kinetics of ivermectin and moxidectin. *Experimental Parasitology* **125**, 172–178.

McConville, M., Hanna, R. E. B., Brennan, G. P., McCoy, M., Edgar, H. W. J., McConnell, S., Castillo, R., Hernández-Campos, A. and Fairweather, I. (2010). *Fasciola hepatica*: disruption of spermatogenesis by the fasciolicide compound alpha. *Parasitology Research* **106**, 311–323.

Meaney, M., Savage, J., Brennan, G. P., Hoey, E., Trudgett, A. and Fairweather, I. (2013). Increased susceptibility of a triclabendazole (TCBZ)-resistant isolate of *Fasciola hepatica* to TCBZ following co-incubation *in vitro* with the P-glycoprotein inhibitor, R(+)-verapamil. *Parasitology* **140**, 1286–1302.

Melaine, N., Liénard, M.-O., Dorval, I., Le Goascogne, C., Lejeune, H. and Jégou, B. (2002). Multidrug resistance genes and P-glycoprotein in the testis of the rat, mouse, guinea pig, and human. *Biology of Reproduction* **67**, 1699–1707.

Messerli, S. M., Kasinathan, R. S., Morgan, W., Spranger, S. and Greenberg, R. M. (2009). *Schistosoma mansoni* P-glycoprotein levels increase in response to praziquantel exposure and correlate with reduced praziquantel susceptibility. *Molecular and Biochemical Parasitology* **167**, 54–59.

Molento, M. B. and Prichard, R. K. (1999). Effects of the multidrug-reversing agents verapamil and CL 347,099 on the efficacy of ivermectin or moxidectin against unselected and drug-selected strains of *Haemonchus contortus* in jirds. *Parasitology Research* **85**, 1007–1011.

Mottier, L., Alvarez, L., Fairweather, I. and Lanusse, C. (2006). Resistance-induced changes in triclabendazole transport in *Fasciola hepatica:* ivermectin reversal effect. *Journal of Parasitology* **6**, 1355–1360.

Pereira, E., Teodori, E., Dei, S., Gualtieri, F. and Garnier-Suillerot, A. (1995). Reversal of multidrug resistance by verapamil analogues. *Biochemical Pharmacology* **50**, 451–457.

Prichard, R. K. and Roulet, A. (2007). ABC transporters and β-tubulin in macrocyclic lactone resistance: prospects for marker development. *Parasitology* **134**, 1123–1132.

Riou, M., Koch, C., Delaleu, B., Berthon, P. and Kerboeuf, D. (2005). Immunolocalisation of an ABC transporter, P-glycoprotein, in the eggshells and cuticles of free-living and parasitic stages of *Haemonchus contortus*. *Parasitology Research* **96**, 142–148.

Robillard, K. R., Hoque, M. T. and Bendayan, R. (2012). Expression of ATP-binding cassette membrane transporters in rodent and human Sertoli cells: relevance to the permeability of antiretroviral therapy at the blood-testis barrier. *Journal of Pharmacology and Experimental Therapeutics* **340**, 96–108.

Robinson, M. W., Trudgett, A., Hoey, E. M. and Fairweather, I. (2002). Triclabendazole-resistant *Fasciola hepatica: β*-tubulin and response to *in vitro* treatment with triclabendazole. *Parasitology* **124**, 325–338.

Robinson, M. W., Lawson, J., Trudgett, A., Hoey, E. M. and Fairweather, I. (2004). The comparative metabolism of triclabendazole sulphoxide by triclabendazole-susceptible and triclabendazole-resistant *Fasciola hepatica*. *Parasitology Research* **92**, 205–210.

Ryan, L., Hoey, E., Trudgett, A., Fairweather, I., Fuchs, M., Robinson, M. W., Chambers, E., Timson, D. J., Ryan, E., Feltwell, T., Ivens, A., Bentley, G. and Johnston, D. (2008). *Fasciola hepatica* expresses multiple α- and β-tubulin isotypes. *Molecular and Biochemical Parasitology* **159**, 73–78.

Savage, J., Meaney, M., Brennan, G. P., Hoey, E., Trudgett, A. and Fairweather, I. (2013*a*). Effect of the P-glycoprotein inhibitor, R(+)-verapamil on the drug susceptibility of a triclabendazole-resistant isolate of *Fasciola hepatica*. *Veterinary Parasitology* **195**, 72–86.

Savage, J., Meaney, M., Brennan, G. P., Hoey, E., Trudgett, A. and Fairweather, I. (2013*b*). Increased action of triclabendazole (TCBZ) *in vitro* against a TCBZ-resistant isolate of *Fasciola hepatica* following its co-incubation with the P-glycoprotein inhibitor, R(+)-verapamil. *Experimental Parasitology* **135**, 642–653.

Scarcella, S., Fiel, C., Guzman, M., Alzola, R., Felipe, A., Hanna, R. E. B., Fairweather, I., McConnell, S. and Solana, H. (2011). Reproductive disruption in *Fasciola hepatica* associated with incomplete efficacy of a new experimental formulation of triclabendazole. *Veterinary Parasitology* **176**, 157–164.

Skuce, P. J. and Fairweather, I. (1988). *Fasciola hepatica*: perturbation of secretory activity in the vitelline cells by the sodium ionophore monensin. *Experimental Parasitology* **65**, 20–30.

Stitt, A. W. and Fairweather, I. (1990). Spermatogenesis and the fine structure of the mature spermatozoon of the liver fluke, *Fasciola hepatica* (Trematoda: Digenea). *Parasitology* **101**, 395–407.

Stitt, A. W. and Fairweather, I. (1991). *Fasciola hepatica*: the effect of the microfilament inhibitor cytochalasin B on the ultrastructure of the adult fluke. *Parasitology Research* **77**, 675–685.

Stitt, A. W. and Fairweather, I. (1992). Spermatogenesis in *Fasciola hepatica*: an ultrastructural comparison of the effects of the anthelmintic, triclabendazole ("Fasinex") and the microtubule inhibitor, tubulozole. *Invertebrate Reproduction and Development* **22**, 139–150.

Stitt, A. W. and Fairweather, I. (1996). *Fasciola hepatica*: disruption of the vitelline cells *in vitro* by the sulphoxide metabolite of triclabendazole. *Parasitology Research* **82**, 333–339.

Stitt, L. E., Tompkins, J. B., Dooley, L. A. and Ardelli, B. F. (2011). ABC transporters influence sensitivity of *Brugia malayi* to moxidectin and have potential roles in drug resistance. *Experimental Parasitology* **129**, 137–144.

Su, L., Mruk, D. D. and Cheng, C. Y. (2011). Drug transporters, the blood-testis barrier and spermatogenesis. *Journal of Endocrinology* **208**, 207–223.

Tiberghien, F. and Loor, F. (1996). Ranking of P-glycoprotein substrates and inhibitors by a calcein-AM fluorometry screening assay. *Anti-Cancer Drugs* **7**, 568–578.

Toffoli, G., Simone, F., Corona, G., Raschack, M., Cappelletto, B., Gigante, M. and Boiocchi, M. (1995). Structure-activity relationship of verapamil analogs and reversal of multidrug resistance. *Biochemical Pharmacology* **50**, 1245–1255.

Tompkins, J. B., Stitt, L. E., Morrissette, A. M. and Ardelli, B. F. (2011). The role of *Brugia malayi* ATP-binding cassette (ABC) transporters in potentiating drug sensitivity. *Parasitology Research* **109**, 1311–1322.

Toner, E., Brennan, G. P., Wells, K., McGeown, J. G. and Fairweather, I. (2008). Physiological and morphological effects of genistein against the liver fluke, *Fasciola hepatica*. *Parasitology* **135**, 1189–1203.

Toner, E., Brennan, G. P., Hanna, R. E. B., Edgar, H. W. J. and Fairweather, I. (2011*a*). Disruption of egg formation by *Fasciola hepatica* following treatment *in vivo* with triclabendazole in the sheep host. *Veterinary Parasitology* **177**, 79–89.

Toner, E., Brennan, G. P., Hanna, R. E. B., Edgar, H. W. J. and Fairweather, I. (2011*b*). *Fasciola hepatica*: time-dependent disruption of spermatogenesis following *in vivo* treatment with triclabendazole. *Parasitology Research* **109**, 1035–1043.

Varma, M. V. S., Ashkraj, Y., Dey, C. S. and Panchagnula, R. (2003). P-glycoprotein inhibitors and their screening: a perspective from bioavailability enhancement. *Pharmacological Research* **48**, 347–359.

Wells, K. (2008). Ion channels and the control of motility in the liver fluke, *Fasciola hepatica*. Ph.D. thesis. The Queen's University of Belfast, Belfast, Northern Ireland.

Wilkinson, R., Law, C. J., Hoey, E. M., Fairweather, I., Brennan, G. P. and Trudgett, A. (2012). An amino acid substitution in *Fasciola hepatica* P-glycoprotein from triclabendazole-resistant and triclabendazole-susceptible populations. *Molecular and Biochemical Parasitology* **186**, 69–72.

Wolstenholme, A. J., Fairweather, I., Prichard, R., Von Samson-Himmelstjerna, G. and Sangster, N. C. (2004). Drug resistance in veterinary helminths. *Trends in Parasitology* **20**, 469–476.

Xu, M., Molento, M., Blackhall, W., Riberio, P., Beech, R. and Prichard, R. (1998). Ivermectin resistance in nematodes may be caused by alteration of P-glycoprotein homolog. *Molecular and Biochemical Parasitology* **91**, 327–335.

Ye, Z. G. and Van Dyke, K. (1988). Reversal of chloroquine resistance in falciparum malaria independent of calcium channels. *Biochemical and Biophysical Research Communications* **30**, 476–481.

https://doi.org/10.1017/S0031182014000377 Published online by Cambridge University Press